

SYNTHESIS OF $\text{Fe}_x\text{Zn}_{1-x}\text{Cr}_2\text{O}_4$ BROWN CERAMIC PIGMENT BY STARCH ASSISTED SOL-GEL PROCESS

Tran Ngoc Tuyen*¹, Nguyen Duc Vu Quyen¹, Tran Bao Lam²

¹Chemistry Department, University of Sciences, Hue University, 77 Nguyen Hue St., Hue, Vietnam

²Nghia Ha Junior High School, Quang Ngai city, Vietnam

Correspondence to Tran Ngoc Tuyen (email: trntuyen@gmail.com)

(Received: 15–5–2019; Accepted: 6–6–2019)

Abstract. In the present paper, the ceramic pigments $\text{Fe}_x\text{Zn}_{1-x}\text{Cr}_2\text{O}_4$ ($x = 0 \div 1$) were synthesized with the starch-assisted sol-gel method. The resulting pigments were characterized using X-ray diffraction (XRD), scanning electron microscopy (SEM), and CIE $L^*a^*b^*$ color measurement. The results show that $\text{Fe}_x\text{Zn}_{1-x}\text{Cr}_2\text{O}_4$ pigments form at sintering temperature of 1100 °C for 60 minutes. The ACr_2O_4 spinel (A: Zn, Fe) and FeCrO_3 perovskite phase with excellent crystallinity appears. The brown color intensity increases gradually with the increase of the number of substituted Fe^{2+} cations. The pigments meet industrial requirements in terms of physicochemical characteristics.

Keywords: brown ceramic pigments, spinel, sol-gel process

1 Introduction

Pigments play an important role in the fabrication of enamel used for ceramic and glass. One of the important physico-mechanical properties of inorganic pigment is the colour fastness at high temperature. Therefore, inorganic pigments are usually synthesized on a stable substrate such as spinel, mullite, cordierite, perovskite, etc. AB_2O_4 spinel has a face-centered cubic lattice formed from O^{2-} anions, where, A^{2+} and B^{3+} cations locates in tetrahedron and octahedron holes, respectively [1]. With a stable crystal structure, spinel has many wonderful physicochemical properties such as high mechanical stability, thermal endurance and chemical durability. ZnCr_2O_4 brown pigment is stable at high temperatures, under light and in chemicals such as acid and base. Therefore, it is usually used to produce: magnetic material [2], ceramic pigments [3, 4], luminescent material [5, 6], gas sensor [7], humidity sensor [6], photocatalyst [8], etc.

ZnCr_2O_4 spinel is mainly synthesized with the traditional ceramic method from ZnO and Cr_2O_3 oxides. In this method, raw materials are mechanically mixed and sintered at high temperature. The product has an unidentical and large size and many phases [9]. To reduce the sintering temperature, ZnCr_2O_4 spinel is currently synthesized with wet methods such as sol-gel [2, 10], precursor method [11], burning [5, 12], co-precipitation [13], ultrasonic and high energy ball milling combined co-precipitation [14], micro-emulsion [7], hydrothermal method [15], hydrothermal combined co-precipitation [16]. The starch-assisted sol-gel process exhibits many advantages such as (i) easy to control the regular proportion of product; (ii) metal cations equally disperse in starch to form a metal-starch complex; (iii) the size of raw material particles are reduced; (iv) contact surface area between reactants is enhanced. This facilitate the solid-phase reaction at low temperature [17].

In the present study, the synthesis of $\text{Fe}_x\text{Zn}_{1-x}\text{Cr}_2\text{O}_4$ ($x = 0 \div 1$) brown pigments by the starch-assisted sol-gel process is shown. The effect of the partly isomorph replacement of Zn^{2+} cations in the tetrahedron holes with Fe^{2+} cations on the color intensity of pigments was demonstrated

2 Experimental

All chemicals employed in the present study are of analytical grade (96-98% purity) from National China Chemical Corporation. ZnCr_2O_4 spinel was synthesized with the sol-gel method from $\text{Zn}(\text{NO}_3)_2 \cdot 6\text{H}_2\text{O}$, $\text{Cr}(\text{NO}_3)_3 \cdot 9\text{H}_2\text{O}$ and dissolved starch. The mixtures of raw materials with a molar ratio of $\text{Zn}^{2+}:\text{Cr}^{3+} = 1:2$, starch: $(\text{Zn}^{2+} + \text{Cr}^{3+}) = 3:5$, $\text{H}_2\text{O}:\text{starch} = 60:1$ were prepared. The mixture was regularly stirred and heated to 60 °C for 1 hour to hydrolyze starch. Then, the mixture was gelatinized at 80-90 °C for 3 hours, and water was evaporated partly to form a more viscous gel of metal-starch precursor. The obtained gel was dried at 100 °C until stable weight. Then, the powder was preheated at 600 °C for 1 hour to decompose the metal-starch precursor, to obtain

highly dispersed metal oxide mixture with an amorphous phase. The mixture of the metal oxides was ground and pressed into a cylinder shape with a diameter of 30 mm and a thickness of 5 mm using the hydraulic press with a compression of 300 kG.cm⁻² (Danir, Denmark). Then, the sample was sintered in a furnace (Lennton, England) at temperatures from 800 to 1100 °C (The samples were coded from ST800 to ST1100) with a heating rate of 10 degrees.min⁻¹ for 1 hour in the air. A sample synthesized at 1100 °C with the traditional method from ZnO and Cr₂O₃ oxide (coded GT1100) was used to assess the effect of the preparation of raw material on the sintering temperature.

In the starch-assisted sol-gel process, the $\text{Fe}_x\text{Zn}_{1-x}\text{Cr}_2\text{O}_4$ pigment was prepared with a partial replacement of Zn^{2+} by Fe^{2+} ($\text{Fe}(\text{NO}_3)_2 \cdot 6\text{H}_2\text{O}$). The effect of Fe^{2+} amount on color intensity was investigated with 10 samples with the x value increasing from 0.1 to 1.0, $(\text{Fe}^{2+} + \text{Zn}^{2+})/\text{Cr}^{3+}$ molar ratio of 0.5, starch/ $(\text{Fe}^{2+} + \text{Zn}^{2+} + \text{Cr}^{3+})$ molar ratio of 0.6, water/starch molar ratio of 60. The sketch of $\text{Fe}_x\text{Zn}_{1-x}\text{Cr}_2\text{O}_4$ synthesis is shown in Fig. 1.

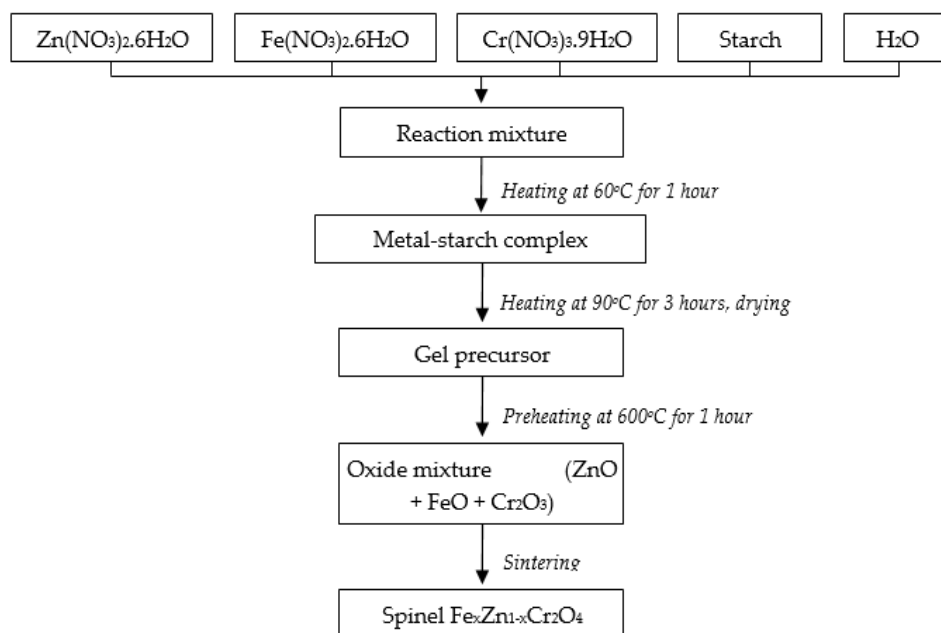


Fig. 1. Diagram of the synthesis of $\text{Fe}_x\text{Zn}_{1-x}\text{Cr}_2\text{O}_4$ pigment by starch assisted sol-gel process

The crystal phase of the sample was determined using X-ray diffraction (XRD) on a Bruker D8 Advance with $\lambda_{\text{Cu-K}\alpha} = 1.5406 \text{ \AA}$. The crystallite size, D , of spinel was calculated using P. Scherrer's equation [17]: $D = \frac{0,9\lambda}{\text{FWHM} \times \cos\theta}$, where λ is the X-ray wavelength (\AA); θ is the diffraction angle (rad) of the (311) peak with the highest intensity and FWHM is the full width at the half maximum of the diffraction peak. The metal-starch complex precursor was characterized using thermal analysis (TG-DSC) on a Labsys TG/DSC Setaram (France) in the ambient air with the maximum temperature of 800 °C and a heating rate of 10 degrees.min⁻¹. The morphology of the obtained sample was studied using scanning electron microscopy (SEM) on a Jeol JSM 5410LV (Japan).

The pigment was used to produce enamel at Vitto Limited Liability Company, Thua Thien Hue. The weight composition of enamel includes 89 % of frit (PT101), 8.9 % of kaolin, 0.1 % of sodium polyphosphate, 0.1 % of carboxyl methyl cellulose and 2 % pigment. The brick after enameling was furnace at 1170 °C for 56 min. The color intensity was measured in color coordination CIE L*a*b* on a Micromath Plus (Instrument, England) at Frit Joint-stock company, Thua Thien Hue. The difference between the two samples was determined as $\Delta E = \sqrt{(L_1^* - L_2^*)^2 + (a_1^* - a_2^*)^2 + (b_1^* - b_2^*)^2}$. The smaller ΔE shows a the more similar color between the two samples.

3 Results and discussion

3.1 Preparation of ZnCr₂O₄ spinel

A weight loss of 18 % (Fig. 2) corresponding to the endothermic peaks at 157 °C may be attributed to the dehydration of starch. The broad exothermal

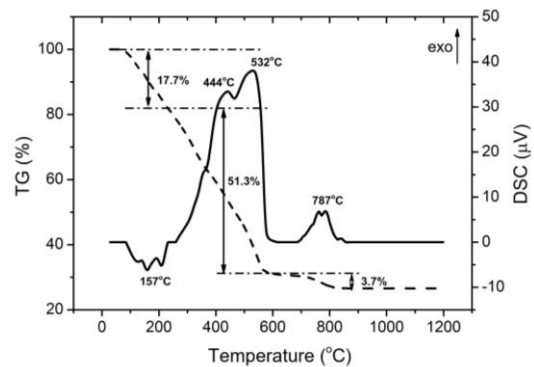


Fig. 2. TG-DSC diagram of ZnCr₂O₄ spinel before sintering

peaks at 444 °C and 532 °C with a weight loss of 51 % may be attributed to the combustion of redundant starch, metal-starch precursor and decomposition of nitrate salts.

The exothermic peak at 787°C refers to the formation of ZnCr₂O₄ crystal from ZnO and Cr₂O₃ formed from the decomposition of the metal-starch precursor. Thus, the temperature of 600 °C and 800 °C are acceptable for the preheating and sintering steps.

Fig. 3 shows the XRD pattern of the pigment samples prepared at sintering temperatures from 800 to 1100 °C. The characteristic diffraction peak at 36.85 ° (311) with a high intensity demonstrates that spinel MgAl₂O₄ forms in all samples. When the sintering temperature increases from 800 to 1100 °C, the intensity of this peak increases from 125 to 242 cps; the FWHM value decreases from 0.499 to 0.300 ° and particle size of the crystal increases from 17 to 28 nm (Table 1). This proves that the crystallization of spinel takes place significantly at 1100°C, and this temperature was chosen for next experiments. The low intensity of diffraction peaks of Cr₂O₃ in the XRD pattern, means that there is a small amount of Cr₂O₃ in the product. Miranda et al. [10] recommended the same sintering temperature when preparing ZnCr₂O₄ by the polymerization of the mixture including glycine, urea and citric acid.

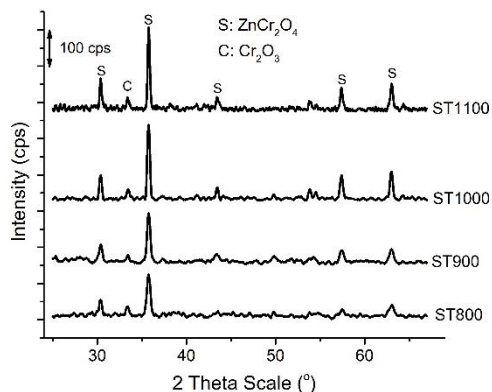


Fig. 3. XRD pattern of ST800, ST900, ST1000 và ST1100 samples

Table 1. Intensity (*I*), FWHM value of diffraction peak and crystal size (*D*) of samples sintered at different temperatures

Sample	FWHM (°)	<i>I</i> (cps)	<i>D</i> (nm)
PEC800	0,499	125	17
PEC900	0,447	144	18
PEC1000	0,376	218	22
PEC1100	0,300	242	28

The XRD patterns of ST1100 and GT1100 are shown in Fig. 4. With the GT1100 sample, the main crystal phase is Cr₂O₃, and the spinel phase appears with low intensity. The solid-phase reaction in the traditional method mostly occurs at more than 1200 °C, which is very high. This demonstrates that the starch-assisted sol-gel method facilitated solid-phase reaction because of the identical distribution of metal oxides [8, 17].

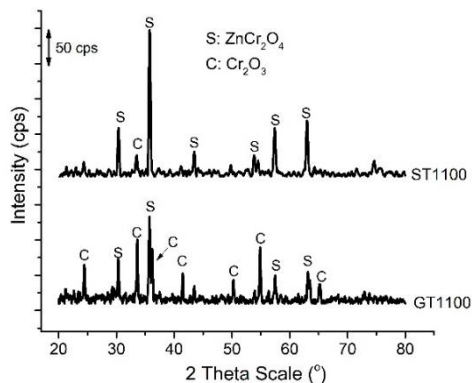


Fig. 4. XRD pattern of ST1100 and GT1100 samples

3.2 Preparation of Fe_xZn_{1-x}Cr₂O₄ pigment

The composition and regular formula of pigment samples, image and color intensity of tile samples after enameling are shown in Table 2 and Fig. 5. It can be seen that the enamel on tiles is brown, smooth with no air bubbles nor disabilities, such as enamel shrink and enamel rift. This demonstrates that the obtained pigment is thermally durable, and the pigment is suitable for the production of enamel. From sample SZ1100 (*x* = 0) to sample SF1100 (*x* = 1), the *L** value decreases from 55.69 to 46.66 and the color changes from light to dark. The *a** value increases from 8.53 to 15.63 and the color changes from green to red. This shows that the color intensity depends on the content of Fe²⁺. The color changes from blue brown to red-brown when increasing the amount of Fe²⁺.

Table 2. Notation and color intensity of Fe_xZn_{1-x}Cr₂O₄ enamel sample

Notation	<i>x</i>	Regular formula	Color intensity		
			<i>L*</i>	<i>a*</i>	<i>b*</i>
SZ1100	0	ZnCr ₂ O ₄	55.96	8.53	12.45
SZF0.1	0.1	Fe _{0.1} Zn _{0.9} Cr ₂ O ₄	54.38	8.96	9.59
SZF0.2	0.2	Fe _{0.2} Zn _{0.8} Cr ₂ O ₄	51.46	9.54	12.11
SZF0.3	0.3	Fe _{0.3} Zn _{0.7} Cr ₂ O ₄	51.35	10.08	14.71
SZF0.4	0.4	Fe _{0.4} Zn _{0.6} Cr ₂ O ₄	51.22	10.53	14.31
SZF0.5	0.5	Fe _{0.5} Zn _{0.5} Cr ₂ O ₄	50.71	10.92	10.92
SZF0.6	0.6	Fe _{0.6} Zn _{0.4} Cr ₂ O ₄	50.16	11.99	12.0
SZF0.7	0.7	Fe _{0.7} Zn _{0.3} Cr ₂ O ₄	49.87	12.75	14.36
SZF0.8	0.8	Fe _{0.8} Zn _{0.2} Cr ₂ O ₄	49.27	13.71	12.11
SZF0.9	0.9	Fe _{0.9} Zn _{0.1} Cr ₂ O ₄	48.45	14.97	13.01
SF1100	1.0	FeCr ₂ O ₄	46.66	15.63	14.82

(*L**: 0 ÷ 100: black ÷ white, *a**: + ÷ - : red ÷ green, *b**: + ÷ - : yellow ÷ dark blue),

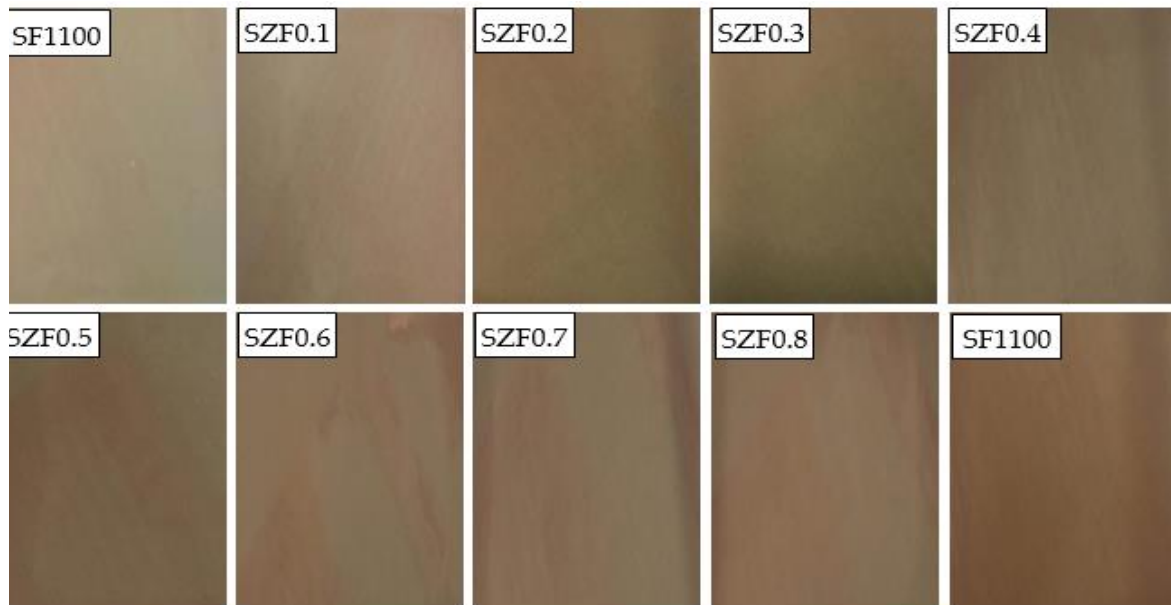


Fig. 5. Tile samples enameled with $\text{Fe}_x\text{Zn}_{1-x}\text{Cr}_2\text{O}_4$ pigment

The XRD pattern of $\text{Fe}_x\text{Zn}_{1-x}\text{Cr}_2\text{O}_4$ pigment (x varying from 0 to 1) is shown in Fig. 6. With sample SZ1100 ($x = 0$) and sample SF1100 ($x = 1$), the main crystal phase is spinel ACr_2O_4 (A: Zn, Fe) with characteristic diffraction peaks at 31.26° , 36.85° , 44.79° , 55.69° and 65.24° corresponding to the (220), (311), (400), (422) and (440) lattice faces. The diffraction peaks corresponding to the (311) lattice plane is high and sharp, which proves good crystallization of spinel. Besides, the diffraction peaks of Cr_2O_3 appear with very low intensity.

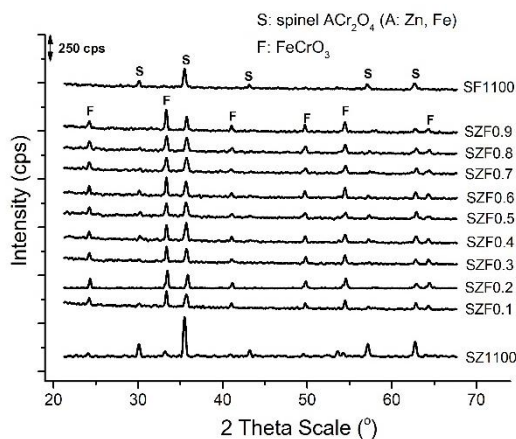


Fig. 6. XRD pattern of $\text{Fe}_x\text{Zn}_{1-x}\text{Cr}_2\text{O}_4$ pigments (x varying from 0 to 1)

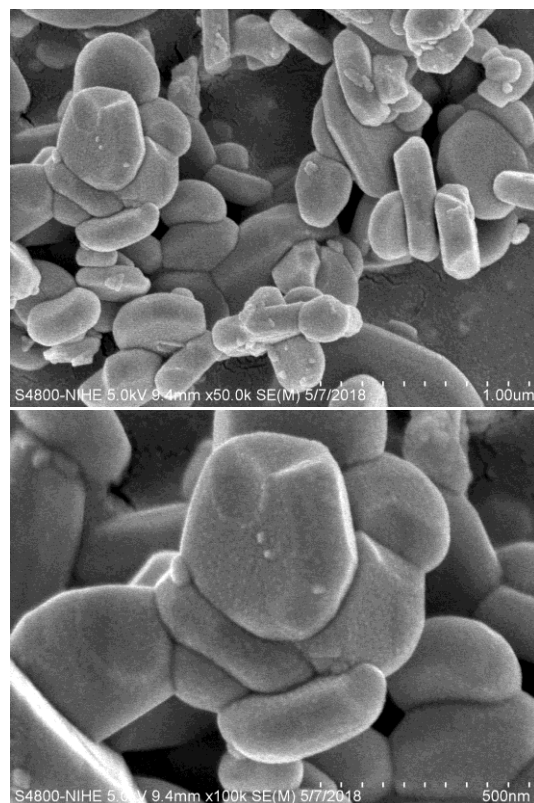


Fig. 7. SEM image of $\text{Fe}_{0.5}\text{Zn}_{0.5}\text{Cr}_2\text{O}_4$ pigment.

When isomorphous Zn^{2+} in the spinel lattice is replaced by Fe^{2+} , the crystal phase composition of the product is multi-phase including spinel and

perovskite FeCrO_3 with strong diffraction peak intensity. This proves that the solid phase reaction between ZnO and Cr_2O_3 or FeO and Cr_2O_3 can form spinel; this reaction between ZnO , FeO and Cr_2O_3 can form both spinel and perovskite.

The morphology and particle size of $\text{Fe}_{0.5}\text{Zn}_{0.5}\text{Cr}_2\text{O}_4$ pigment prepared at $1100\text{ }^\circ\text{C}$ for 60 min (Fig. 7) show that the product has a uniform particle size with a diameter varying from 280 to 420 nm. The particles do not agglomerate into a large bulk and the boundary between particles is clear. The nanometer-sized pigment synthesized with the starch-assisted sol-gel method can be used in the pigment inkjet technology onto the surface of the product that is a current hot topic in ceramic production [10].

4 Conclusion

$\text{Fe}_x\text{Zn}_{1-x}\text{Cr}_2\text{O}_4$ pigments (x varying from 0 to 1) were successfully synthesized with the starch-assisted sol-gel method. The suitable sintering temperature is $1100\text{ }^\circ\text{C}$ which is lower than that of the traditional method. The obtained product exhibits the main crystal phase of spinel, where x is 0 and x is 1. When $0 < x < 1$, the perovskite phase appears beside spinel. The enamel on tiles is brown, smooth with no air bubbles nor disabilities, such as enamel shrink and enamel rift. The color depends on the amount of iron. The pigment is suitable for the production of enamel and meets the industrial requirements of ceramic production.

References

1. Shackelford JF, Alexander W. *Materials Science and Engineering Handbook*. CRC Press. 2001
2. Chen XH, Zhang HT, Wang CH, Luo XG, Li PH. Effect of particle size on magnetic properties of zinc chromite synthesized by sol-gel method. *Applied Physics Letters*. 2002;81(23):4419-4421.
3. Fiuza TER, Gottert D, Pereira LJ, Antunes SRM, Andrade AVC, Antunes AC, Souza ECF. Production of brown inorganic pigments with spinel structure using spent zinc-carbon batteries. *Processing and Application of Ceramics*. 2018;12(4):319-325.
4. Milanez KW, Kuhnen NC, Riella HG, Knies CT. Obtaining of ceramics pigments $(\text{Fe}, \text{Zn})\text{Cr}_2\text{O}_4$ using waste of electroplating as raw material. *Materials Science Forum*. 2005;498-499:654-657.
5. Ghosh D, Dutta U, Haque A, Mordvinova NE, Lebedev OI, Pal K, Gayen A, Seikh M, Mahata P. Ultra high sensitivity of luminescent ZnCr_2O_4 nanoparticles toward aromatic nitro explosives sensing. *Dalton Transactions*. 2018;14:1-18.
6. Singh N, Rhee JY. Electronic structures and optical properties of Spinel ZnCr_2O_4 . *Journal of the Korean Physical Society*. 2010;57(5):1233-1237.
7. Niu X, Du W, Du W. Preparation and gas sensing properties of ZnM_2O_4 ($M = \text{Fe}, \text{Co}, \text{Cr}$). *Sensors and Actuators*. 2004;B99:405-409.
8. Yazdanbakhsh M, Khosravi I, Goharshadi EK, Youssefi A. Fabrication of nanospinel ZnCr_2O_4 using sol-gel method and its application on removal of azo dye from aqueous solution. *Journal of Hazardous Materials*. 2010;684-689.
9. Marinkovic ZV, Mancic L, Vulic P, Milosevic O. The influence of mechanical activation on the stoichiometry and defect structure of a sintered $\text{ZnO-Cr}_2\text{O}_3$ system. *Materials Science Forum Online*. 2004;453-454:423-428.
10. Miranda EAC, Carvajal JFM, Baena OJR. Effect of the fuels glycine, urea and citric acid on synthesis of the ceramic pigment ZnCr_2O_4 by solution combustion. *Materials Research*. 2015;18(5):1038-1043.
11. Gingasu D, Mindru I, Patron L, Culita DC, Moreno MC, Diamandescu L, Feder M, Oprea O. Precursor method—A nonconventional route for the synthesis of ZnCr_2O_4 spinel. *Journal of Physics and Chemistry of Solids*. 2013;74:1295-1302.
12. Khetre SM, Chopade AU, Jadhav HV, Kulal SR, Jagadale PN, Bangale SV. Auto-combustion synthesis of nanocrystalline FeCrO_3 , *International Conference on Nanoscience. Technology and Societal Implications*. 2011.
13. Mousavi Z, Soofiand F, Zare ME, Niasari MS, Bagheri S. ZnCr_2O_4 nanoparticles: facile synthesis, characterization, and photocatalytic properties. *Scientific Reports*. 2016:1-11.
14. Nieves LJJ, Baena OJR, Tobon JI. Synthesis of ceramic pigments ACr_2O_4 using the non-

- conventional method of co-precipitation assisted by ultrasound and high energy milling. *Open Journal of Inorganic Non-Metallic Materials*. 2014;4:54-63.
15. Peng C, Gao L. Optical and photocatalytic properties of spinel $ZnCr_2O_4$ nanoparticles synthesized by a hydrothermal route. *Journal of the American Ceramic Society*. 2008;91(7):2388-2390.
 16. Tajizadegan H, Heidary A, Torabi O, Golabgir MH, Jamshidi A. Synthesis and characterization of $ZnCr_2O_4$ nanospinel prepared via homogeneous precipitation using urea hydrolysis. *International Journal of Applied Ceramic Technology*. 2016;13(2):289-294.
 17. Kofenstein R, Walther T, Hesse D, Ebbinghaus SG. Preparation and characterization of nanosized magnesium ferrite powders by a starch-gel process and corresponding ceramics. *Journal of Materials Science*. 2013;48:6509-6518.